Earth's Future

RESEARCH ARTICLE
10.1029/2024EF004431

High-Resolution Modeling and Projecting Local Dynamics of Differential Vulnerability to Urban Heat Stress

I. Marginean[1,2], J. Crespo Cuaresma[3,4,5], R. Hoffmann[4], R. Muttarak[6], J. Gao[7], and Anne Sophie Daloz[1]

[1]CICERO Center for International Climate Research, Oslo, Norway, [2]Department of Geosciences, Meteorology and Oceanography Section, University of Oslo, Oslo, Norway, [3]Department of Economics, WU Vienna University of Economics and Business, Vienna, Austria, [4]International Institute for Applied Systems Analysis (IIASA), Laxenburg, Austria, [5]Austrian Institute of Economic Research, Vienna, Austria, [6]Department of Statistical Sciences "Paolo Fortunati", University of Bologna, Bologna, Italy, [7]Department of Geography and Spatial Sciences & Data Science Institute, University of Delaware, Newark, DE, USA

Key Points:

- Population projections by age, sex and education at small-area levels allow for high-resolution heat vulnerability modeling
- Vulnerability to heat stress can vary widely between different areas in a city, and even within a single neighborhood
- Areas that are vulnerable today are projected to become even more vulnerable in all Shared Socioeconomic Pathway scenarios except for that assuming a sustainable development narrative

Supporting Information:

Supporting Information may be found in the online version of this article.

Correspondence to:

I. Marginean,
iulia.marginean@cicero.oslo.no

Citation:

Marginean, I., Crespo Cuaresma, J., Hoffmann, R., Muttarak, R., Gao, J., & Daloz, A. S. (2024). High-resolution modeling and projecting local dynamics of differential vulnerability to urban heat stress. *Earth's Future*, *12*, e2024EF004431. https://doi.org/10.1029/2024EF004431

Received 8 JAN 2024
Accepted 6 SEP 2024

Author Contributions:

Conceptualization: I. Marginean, J. Crespo Cuaresma, R. Muttarak, J. Gao
Data curation: I. Marginean
Formal analysis: I. Marginean, R. Hoffmann
Funding acquisition: I. Marginean
Investigation: I. Marginean, R. Hoffmann
Methodology: I. Marginean, J. Crespo Cuaresma
Project administration: I. Marginean
Resources: I. Marginean

© 2024. The Author(s).
This is an open access article under the terms of the Creative Commons Attribution-NonCommercial-NoDerivs License, which permits use and distribution in any medium, provided the original work is properly cited, the use is non-commercial and no modifications or adaptations are made.

Abstract Climate change-induced heat stress has significant effects on human health, and is influenced by a wide variety of factors. Most assessments of future heat-related risks however are based on coarse resolution projections of heat hazards and overlook the contribution of relevant factors other than climate change to the negative impacts on health. Research highlights sociodemographic disparities related to heat stress vulnerability, especially among older adults, women and individuals with low socioeconomic status, leading to higher morbidity and mortality rates. There is thus an urgent need for detailed, local information on demographic characteristics underlying vulnerability with refined spatial resolution. This study aims to address the research gaps by presenting a new population projection exercise at high-resolution based on the Bayesian modeling framework for the case study of Madrid, using demographic data under the scenarios compatible with the Shared Socioeconomic Pathways. We examine the spatial and temporal distribution of population subgroups at the intra-urban level within Madrid. Our findings reveal a concentration of vulnerable populations, as measured by their age, sex and educational attainment level in some of the city's most disadvantaged neighborhoods. These vulnerable clusters are projected to widen in the future unless a sustainable trajectory is realized, driving vulnerability dynamics toward a more uniform and resilient change. These results can guide local adaptation efforts and support climate justice initiatives to protect vulnerable communities in urban environments.

Plain Language Summary Heat stress is a major risk factor for human health, especially in cities where more people are exposed to increasingly higher temperatures in summer. Cities are usually hotter than their surrounding rural areas due to the predominance of dark, impervious surfaces which absorb more heat. Assessing heat risks for public health requires measurements of the hazard, such as a prolonged period with high temperatures, the population exposed to the hazard and characteristics of populations that make them more vulnerable to heat related diseases or even death. Various approaches and tools for risk assessment have been developed, but most of them focus on the hazard and exposure components. In this paper, we measure and project vulnerability to heat stress in alternative scenarios, using different population characteristics, such as age, sex and education. Our results show that there are compelling differences between areas within the city of Madrid and that areas that are vulnerable today will become even more vulnerable unless we follow a path of sustainable development. Detailed assessments of the spatial distribution of vulnerability within a city are relevant for developing adaptation solutions that target vulnerable populations and are thus more effective in reducing heat-related risks.

1. Introduction

Climate change has severe impacts on human health worldwide. The direct effects of heat stress associated with the warming climate manifest through increasing disease and premature death rates (Ebi et al., 2018; Gasparrini et al., 2017; Honda et al., 2014). Already, over one third of warm-season heat-related deaths can be attributed to anthropogenic climate change (Vicedo-Cabrera et al., 2021). These effects are most visible in cities, where more people are exposed to temperatures that are significantly higher than in their surrounding rural areas (Hsu et al., 2021). Without appropriate adaptation strategies, the already notable health impacts will intensify rapidly in

Supervision: J. Crespo Cuaresma, R. Muttarak, J. Gao, Anne Sophie Daloz
Validation: I. Marginean
Visualization: I. Marginean, R. Hoffmann, Anne Sophie Daloz
Writing – original draft: I. Marginean, J. Crespo Cuaresma
Writing – review & editing: I. Marginean, J. Crespo Cuaresma, R. Muttarak, Anne Sophie Daloz

the future urban environments under global warming (Zhao et al., 2021). The increased exposure to hazards may go hand in hand with an increase in overall vulnerability due to projected urbanization (Jiang & O'Neill, 2017) and aging of urban populations (Jay et al., 2021).

The latest report from the Intergovernamental Panel on Climate Change (IPCC) highlights that vulnerability is potentially a more important driver of severe climate risks than global warming levels (O'Neill et al., 2022). Even if we achieve the goals of the Paris Agreement and contain warming well below 2°C, striving to limit the warming to 1.5°C above pre-industrial levels, through strong mitigation efforts, the risk of heat stress will remain moderate to high in scenarios with limited or incomplete adaptation and only a pro-active adaptation scenario will keep the risks within moderate limits (Cisse et al., 2022). Effective adaptation solutions are those that target the groups that are most affected by the negative impacts of climate change and increase their resilience. Therefore, the severity of future climate change impacts will be highly dependent on how efficiently vulnerability can be decreased (Begum et al., 2022). Despite this insight, the scientific community as well as policy makers have focused almost exclusively on trends of heat hazards, with little to no research being conducted on how societal change influences vulnerability dynamics (Garschagen et al., 2021). We address this gap by modeling and projecting local changes in heat-related vulnerability in alternative scenarios at a very high spatial resolution for the case of Madrid.

Vulnerability is defined as the predisposition of individuals, communities or systems to be disproportionately affected by climate change impacts, due to heightened sensitivity and diminished adaptive capacity. Different approaches have been used over time to assess vulnerability. Early analyses took a top-down, biophysical perspective which often started with exposure to climate hazards. Over time, this evolved into a bottom-up evaluation, accounting for social and contextual determinants of vulnerability. Vulnerability is a core component of climate risk and often assessed in relation to hazards and exposure, but studied on its own, it can improve our understanding of differential impacts based on societal and individual characteristics of the affected populations. The approach provides a unique lens to study the effects of heat stress on different communities and individuals and assesses how these are affected by race, gender, wealth inequalities and other attributes (Begum et al., 2022). Demographic and socioeconomic factors as well as preexisting health conditions shape vulnerability in complex ways. Old age, with its related health conditions is one of the strongest determinants of heat stress vulnerability (Benmarhnia et al., 2015; López-Bueno et al., 2020). In general, women are shown to be more susceptible to heat than men, but these results vary with location. A recent systematic literature review of 207 studies found 37 articles showing higher risk for women and 12 articles showing higher risk for men (Son et al., 2019). Living alone increases the risk of mortality and so does living in a low-income household (Osberghaus & Thomas, 2022) and having a low level of education (Conte Keivabu, 2022).

Societal change and its effects on future vulnerability have been largely overlooked by the existing literature, but recently, several contributions emphasize the need for a better integration of vulnerability aspects in future climate risk assessments. This realization has led to the development of a new scenario architecture that considers such socioeconomic changes in climate change science (Garschagen et al., 2021). The Shared Socioeconomic Pathways (SSPs) are the latest generation of scenarios that integrate potential changes in future climate with societal development. This set of five scenarios provides global data on trajectories for climate change as well as economic and demographic development (O'Neill et al., 2017). These data are seldom used by local decision makers due to a mismatch in the spatial scales between the socioeconomic projections and the information relevant for decision making, for example, in a municipal context. The modeling tools and methods available today are insufficient to achieve the level of resolution required to accurately model vulnerability and adaptation scenarios for a geographical area as small as a city (Garschagen et al., 2021).The climate research community has made sustained efforts to downscale data from global climate models to regional (CORDEX Regional Climate Model Data on Single Levels, 2019) and local contexts (Fick & Hijmans, 2017), and even developed high resolution products for detailed urban modeling (Copernicus Climate Change Service, 2019) with a wide range of tools available for statistical or dynamical downscaling. At the same time, only limited downscaled projections exist for data on vulnerability in local contexts. We address this gap by developing a framework for downscaling socioeconomic data from the SSPs at scales that are useful for local decision-making.

The following section presents an overview of the background and research gaps addressed in this article, then Section 3 outlines the data and methods while Section 4 summarizes the results and Section 5 discusses the limitations and provides concluding remarks.

23284277, 2024, 10, Downloaded from https://agupubs.onlinelibrary.wiley.com/doi/10.1029/2024EF004431 by Area Sistemi Dipart & Document, Wiley Online Library on [23/10/2024]. See the Terms and Conditions (https://onlinelibrary.wiley.com/terms-and-conditions) on Wiley Online Library for rules of use; OA articles are governed by the applicable Creative Commons License

23284277, 2024, 10, Downloaded from https://agupubs.onlinelibrary.wiley.com/doi/10.1029/2024EF004431 by Area Sistemi Dipart & Document, Wiley Online Library on [23/10/2024]. See the Terms and Conditions (https://onlinelibrary.wiley.com/terms-and-conditions) on Wiley Online Library for rules of use; OA articles are governed by the applicable Creative Commons License

2. Knowledge Gaps in Heat-Related Vulnerability

Local assessments of vulnerability are often the first step in identifying challenges and opportunities for mapping health risks related to climate change (Haines & Ebi, 2019). Most future heat-related risk assessments are based on changes in heat hazards while socioeconomic factors are kept constant, at the current conditions. The future vulnerability of populations in cities will be determined by how society and the characteristics of urban population develop in the years to come, but the contribution of drivers of urban heat stress, other than climate change are widely neglected in future risk assessments (Rohat et al., 2019). Socioeconomic scenarios have been developed to address this drawback and play a key role in the assessment of future heat stress risks as well as in the design of adaptation policy responses (Riahi et al., 2017). To this end, the SSPs, which comprise a set of five coherent narratives, are useful to describe plausible future changes in demographics, economics, human development, policies and institutions, technology, and environment and natural resources (O'Neill et al., 2017). The demographic component of the SSPs provides a powerful resource for analyzing population dynamics according to different assumptions about future trends in population structure, fertility, mortality and migration. In this work, we develop high-resolution projections that follow three of the five SSPs, namely SSP1—"sustainable development", SSP2—"middle-of-the-road" and SSP3—"regional rivalry."

Demographically, SSP1 assumes a future of sustainable development where investments in health and education lead to a relatively low global population, with low mortality, medium fertility and migration and high education. Overall fertility in this scenario is medium, due to the assumption that in rich OECD countries, the strong focus on wellbeing is making it easier for women to combine work and family life while in all other countries, fertility remains low. SSP2, the middle-of-the-road scenario, carries the trends from the recent past well into the future, following a medium mortality, fertility, migration and education trajectory. In stark contrast to SSP1, the SSP3 scenario describes a fragmented world dominated by conflict, where increasing nationalistic sentiments and high investments in national security hinder efforts for international cooperation and sustainability. Turmoil in this world leads to high mortality and low educational attainment, which result in high fertility rates. Furthermore, due to security and barriers for international exchange, migration remains low (KC & Lutz, 2017). Within health systems, SSP1 assumes strong climate change and health planning in governance, with well-developed health information systems that focus on vulnerability assessments and investments in research of vulnerable communities. SSP2 includes some governance on climate change and health, but planning and vulnerability assessments are not always prioritized or comprehensive due to political and financial constraints. SSP3 assumes minimal to no planning regarding climate change and health issues. Vulnerability assessments are rarely conducted and weak climate financing systems restrict adaptation activities (Haines & Ebi, 2019). Using the SSP trajectories for future climate and health vulnerability assessments offer unique advantages of combining the demographic projections as vulnerability factors with the climate scenarios. The Sixth Assessment Report of the IPCC (AR6) provides a framework for integrating the socioeconomic aspects of future development with a range of radiative forcing values that would occur in alternative climates. The SSPs as described above, can be combined with an older generation of climate scenarios, namely the representative concentration pathways (RCPs) which imply different magnitudes of warming, expressed by the level of radiative forcing that they would potentially reach in 2100. Examples of potential combinations are SSP1-1.9 - a low overshoot scenario consistent with limiting global average warming to 1.5°C by 2100, SSP1-2.6 - a scenario consistent with limiting warming to 2°C, SSP2-4.5—consistent with a warming in the range of 2.1°C–3.5°C or SSP3-7.0 consistent with warming in the range of 2.8°C–4.6°C (Begum et al., 2022). The demographic projections (KC & Lutz, 2017), however, do not explicitly assume effects of climatic events on the drivers of population change and have thus been developed independently of the climate projections. Furthermore, a lack of quantitative and spatially explicit projections of socioeconomic variables under the SSPs is one of the key barriers to integrating socioeconomic scenarios within local climate risk assessments (Rohat et al., 2019). Studies applying the SSP scenario framework have used coarse resolutions, such as 0.5° spatial grids (e.g., Liu et al., 2017). The high-resolution, spatially explicit and demographically heterogeneous population projections that we developed in this paper are readily available to be integrated in more complex heat-related risk assessments.

Our choice to use demographic variables (i.e., age, sex, and education) to quantify future vulnerability is supported by previous studies, which have found these variables to significantly modify the heat-mortality relationship due to both physiological and behavioral differences. Literature shows that individuals above the age of 65, those with low socioeconomic status (SES) and women are more susceptible to heat-related illnesses and mortality (Basu, 2009; Benmarhnia et al., 2015; Conlon et al., 2020; Son et al., 2019; Stafoggia et al., 2021).

23284277, 2024, 10, Downloaded from https://agupubs.onlinelibrary.wiley.com/doi/10.1029/2024EF004431 by Area Sistemi Dipart & Document, Wiley Online Library on [23/10/2024]. See the Terms and Conditions (https://onlinelibrary.wiley.com/terms-and-conditions) on Wiley Online Library for rules of use; OA articles are governed by the applicable Creative Commons License

Research consistently underscores that age is the most prevalent factor modifying the relationship between ambient temperature and mortality given that older people have a reduced ability to thermoregulate their body temperature, higher prevalence of underlying health conditions, tendency to live alone and limited access to medical care and social services (Son et al., 2019). Sex is also considered a source of demographic heterogeneity underlined by differences in physiology and exposure (Achebak et al., 2019; Oudin Åström et al., 2011). There is however no consensus on whether men or women are more vulnerable to heat stress, with slightly higher number of studies reporting women to have higher mortality risks (Son, Liu, and Bell, 2019).

In recent years, education has been put forward as an important demographic characteristic underlying vulnerability to climate change and adaptive capacity (Conte Keivabu, 2022; Lutz et al., 2014; Muttarak, 2021; Muttarak & Lutz, 2014). It has been consistently shown that individuals, households, communities and countries with higher level of education experience lower vulnerability to extreme climatic events measured as mortality, morbidity, loss and damages and recovery time (Butz et al., 2014). There are two main channels underlying the role of education in reducing vulnerability and enhancing adaptive capacity. First, formal schooling directly enhances risk perception, problem solving skills and cognitive skills such as inductive reasoning (Van Vo & Csapó, 2020) and working memory, which is responsible for storing and manipulating information necessary for complex cognitive tasks (Davidson et al., 2023). These qualities are useful to prepare for and cope with climatic risks. Hoffmann and Muttarak (2017) for instance, show that individuals with more years of schooling have different levels of risk perception and this partially explains why they have higher level of disaster preparedness. In certain circumstances, a positive link between education and risk attitudes is shown to be causal (Chong & Martinez, 2021). Likewise, Dimitrova and Muttarak (2020) find that more educated mothers in India have better health knowledge and access to healthcare services enabling them to protect their children against malnourishment after floods exposure. Furthermore, individuals with higher level of education also have higher and better access to social and economic resources and social networks.

It has been reported that individuals with higher level of education generally have lower mortality risks from extreme temperatures (both hot and cold) (Conte Keivabu 2022; Lloyd et al., 2023; Schneider et al., 2022). This is partly because low-educated individuals often live in poor housing conditions with inadequate insulation and limited cooling and heating systems (Min et al., 2021). Given that education is highly relevant in determining vulnerability, in this study, we explicitly incorporate education as a key source of demographic heterogeneity.

Another aspect requiring attention is our understanding of the spatial distribution of heat-related risks and heat stress within cities. Heat stress intensity varies greatly from one neighborhood to another and even within the neighborhoods of one city. Yet, most studies quantifying the relationship between ambient air temperature and health outcomes lack granularity. Exposure-response relationships are generally estimated on city-wide data (Gasparrini et al., 2015), with only a handful investigating the differences within urban areas (Smargiassi et al., 2009; Zafeiratou et al., 2019). Identification of vulnerable intra-urban areas and the formulating prevention and response strategies within local adaptation plans that specifically target these areas are essential steps in reducing the health burden caused by heat stress in urban environments (Benmarhnia et al., 2015; Schneider et al., 2022). Analyzing population distribution and dynamics at the intra-urban scale helps quantify these differential risks (Piel et al., 2020). Thus, conducting analysis at a more granular spatial resolution plays a pivotal role in enhancing the effectiveness of local adaptation policies. These insights are essential for crafting public health adaptation strategies that are tailored to the specific needs in the local context, as opposed to relying exclusively on national-level policy development. Nevertheless, while high resolution climate modeling and downscaling of heat hazard data are well established approaches (e.g., Smid & Costa, 2018), local vulnerability assessments and downscaling of vulnerability data is only now emerging as a topic in climate risk studies. The few published studies develop their own scenarios using mixed methods and data from interviews with local stakeholders as well as quantitative vulnerability metrics (e.g., Birkmann et al., 2021). Population projections are computations of future populations based on assumptions about drivers of demographic changes, without any associated probabilities regarding their likelihood. Population projections at the national and large subnational scales have generally benefitted from far more extensive research on methods and data preparation. While methods for small area projections such as downscaling and disaggregation approaches, microsimulation and machine learning exist, they remain little developed over the past years (Wilson et al., 2022). Likewise, well-established methods for coarse-resolution projections are not always suited at higher resolution because the latter are likely to suffer from population forecast errors. Standard cohort-component models (CCMs) are a

23284277, 2024, 10, Downloaded from https://agupubs.onlinelibrary.wiley.com/doi/10.1029/2024EF004431 by Area Sistemi Dipart & Document, Wiley Online Library on [23/10/2024]. See the Terms and Conditions (https://onlinelibrary.wiley.com/terms-and-conditions) on Wiley Online Library for rules of use; OA articles are governed by the applicable Creative Commons License

common tool for producing population projections but they are not necessarily suited for all types of projections. CCMs require data on the three main components of demographic change - fertility, mortality and migration that are disaggregated by the dimensionality of the population projections. Some of these demographic variables are not always available at high resolutions (Hauer, 2019). They also present difficulties capturing population heterogeneity in the context of changes in the dwelling stock in growing urban areas. Furthermore, they are ill-suited for handling multidimensional data, and differentiate between influences of different conditions (Puga-Gonzalez et al., 2022). Model averaging approaches have been long used in statistics and forecasting literature, but they are not commonly used in demographic projections. Nevertheless, they are found to perform well for small area population forecasts and reduce errors. In particular, Bayesian methods can be particularly useful with small area projections because they require little input data compared to frequentist approaches, allow for inclusion of prior assumptions related to demographic changes and can combine data from different sources, dealing well with missing data (Wilson et al., 2022).

As argued above, age, sex and education are important sources of population heterogeneity, and their changing composition is directly relevant for vulnerability reduction and adaptation to climate change (KC & Lutz, 2017). However, datasets of population projections that are stratified by age, sex and education and compatible with the SSP narratives are available only at country level. Higher resolution global population data at one-eighth of a degree (Jones et al., 2020) and 1 km grids (Gao, 2017) are also available at decadal time intervals for the 21st century but the data are aggregated at the total population level, split between urban and rural status. Although the latter are valuable data for assessing increased exposure within urban areas, they do not provide enough information for quantifying individual biophysical and social vulnerabilities at the intra-urban level. This lack of granular data leads to research on adaptation to heat stress consisting mostly of studies carried out at the regional or national scale. Such coarse resolutions may mask differences in vulnerabilities of certain population subgroups and smaller areas. Assessing and projecting demographically differentiated vulnerability at intra-urban scales is essential to improve our understanding of current and future climate risks from heat stress (Muttarak, 2021). In this respect, downscaling coarse resolution demographic data is key to supporting local decision-makers in designing solutions specifically targeting the most vulnerable groups.

Developing a spatial and demographically explicit vulnerability modeling framework is an important first step toward designing adaptive strategies targeting vulnerable groups in cities. This paper addresses two major research gaps concerning heat-related risk quantification and its spatial-temporal distribution. First, we provide an accessible approach to quantify vulnerability by using demographic characteristics of the population (Basu, 2009; Calleja-Agius et al., 2021; Conlon et al., 2020; Jurgilevich et al., 2017; Muttarak, 2021). Second, we address the need for detailed, high-resolution vulnerability data, differentiated by demographic dimensions such as age, sex and education at fine geographical resolution (Gao, 2017; Wear & Prestemon, 2019; Zoraghein & Brian, 2020) and develop granular projections that are aligned with the SSPs. The implementation of this framework is intended on a city-by-city basis, as endeavors to conduct a comprehensive assessment across broader regions, may inadvertently disregard nuanced risks present within smaller localized areas of a city. As a demonstration of its applicability, we present the case study conducted in Madrid, Spain and encourage its replicability in other cities.

This paper adopts the conceptualization of risk described in the AR6 (Begum et al., 2022), which defines heat-related risk as a combination of heat hazards (temperatures that are high enough to cause negative health responses such as morbidity or mortality), exposure to these hazards (presence of people) and vulnerability of the population (a combination between sensitivity—characterized by a wide variety of sociodemographic factors—and adaptive capacity—the populations' ability to prepare, respond to and recover from heat-related hazards).

3. Methods

In this paper, we develop a new tool to obtain high-resolution, spatially explicit projections of demographic variables that are relevant for future vulnerability assessments. To achieve this, we collect population data stratified by age, sex and education at the highest resolution available (census tract) for Madrid. We exploit the characteristics of the rate of change and convergence rates for the shares of population by educational attainment from the three global SSPs in order to obtain decadal projections at the census tract level in Madrid and thus create spatial high resolution data at decadal intervals, aligned with three SSP scenarios (SSP1—"sustainable development", SSP2—"middle-of-the-road" and SSP3—"regional rivalry"). We explicitly address specification

10.1029/2024EF004431

23284277, 2024, 10, Downloaded from https://agupubs.onlinelibrary.wiley.com/doi/10.1029/2024EF004431 by Area Sistemi Dipart & Document, Wiley Online Library on [23/10/2024]. See the Terms and Conditions (https://onlinelibrary.wiley.com/terms-and-conditions) on Wiley Online Library for rules of use; OA articles are governed by the applicable Creative Commons License

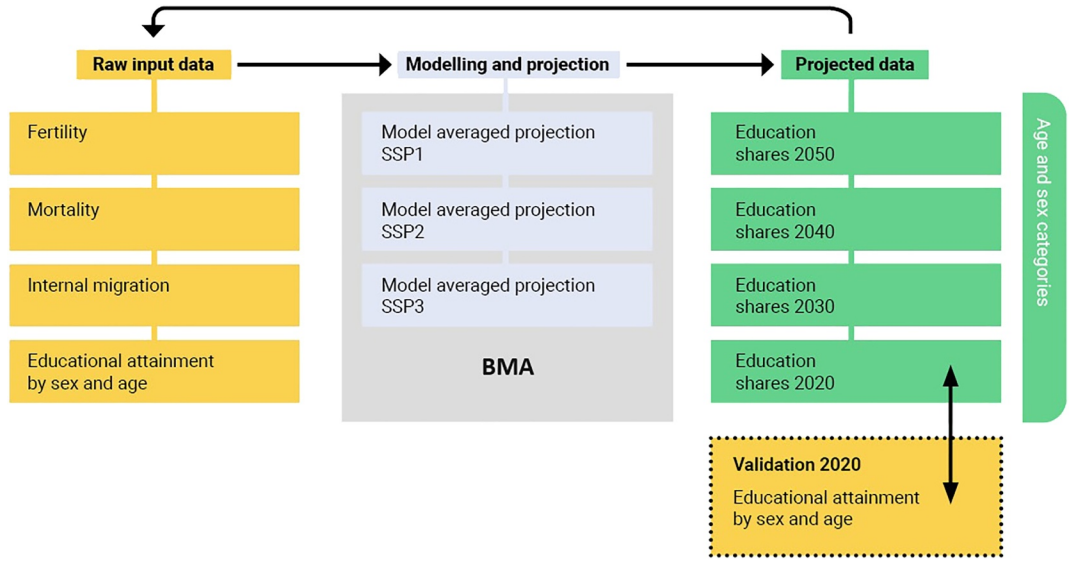

Figure 1. Conceptual figure of the main relations between the model input (yellow boxes) and output data, projection model runs for the three SSP scenarios (gray boxes), and model outputs (green boxes). The models use baseline fertility, mortality, migration, and education data to project age, sex, and education compositions by SSPs at a high spatial resolution at the census tract level. Educational attainment by sex and age refers to raw education data and Education shares, followed by the year refers to projected education data.

uncertainty in the projection exercise using Bayesian model averaging (BMA). We limit the projections to population changes aligned with the demographic trends of the SSPs, omitting other socioeconomic variables due to the lack of high-resolution raw data for the latter. While the demographic data, stratified by age, sex, and education, are available at the census tract level, the economic data, which could have been adapted to correspond with the economic component of the SSPs, only exist at the coarser district level.

We use BMA to investigate the empirical drivers of changes in the shares of population stratified by age, sex and educational attainment. We apply BMA on linear regression models for the change in shares between 2012 and 2020 for each of the 18 age-sex-education categories defined by the two sexes, three age groups (25–64, 65–84 and 85+) and three educational attainment levels (low, medium and high). We then compute projections for the three scenarios based on the coefficient estimates obtained from the model averaging exercise. The predictions for 2020 are compared to observations data at the same resolution (census tract) for model validation. We employ decadal values of age-specific fertility and mortality projections in Spain by SSP scenario, while keeping internal migration constant, since the SSP scenarios contain narratives on international migration but not for populations mobility within cities. Imposing these scenario trajectories on the developments of population drivers, we obtain projections of the shares of population by age, sex and educational attainment up to 2050.

Conceptual Figure 1 outlines the modeling framework. The model input data (yellow boxes) consists of fertility, mortality and internal migration together with population data at census tract resolution for the years 2012 and 2020, grouped by sex: males and females, for three age categories: 25–64, 65–84 and 85+ years of age, and three education categories: low, medium and high. We run BMA for each age, sex and education category individually, with the 2020 shares of each education category (bottom yellow box in the Raw input data section in Figure 1) as the dependent variable and with 2012 shares of all three education categories, in addition to fertility, mortality and migration shares for 2010 as independent variables. For SSP2 (middle gray box in the Modeling and projection section in Figure 1), we create model averaged projections for the shares on each education category in 2020 (bottom green box in the Projected data section in Figure 1), based on the BMA estimates and the realized values of the six independent variables described above. We compare the projected education shares in 2020 with the observed, raw data from the same year to validate our method. The comparison is represented by the double-edged arrow between the yellow box in the bottom right corner and bottom green box in the Projected data section in Figure 1. We then use the raw 2020 data for education shares and the mortality and fertility projections for 2020 as well as migration shares (see Supplementary Text S2 in Supporting Information S1 for a more detailed description

23284277, 2024, 10, Downloaded from https://agupubs.onlinelibrary.wiley.com/doi/10.1029/2024EF004431 by Area Sistemi Dipart & Document, Wiley Online Library on [23/10/2024]. See the Terms and Conditions (https://onlinelibrary.wiley.com/terms-and-conditions) on Wiley Online Library for rules of use; OA articles are governed by the applicable Creative Commons License

of fertility, mortality and migration data preprocessing) to create projections of education categories for 2030. The 2030 projections are again used as input to project 2040 data and the same procedure is repeated for 2050 projections, using 2040 data as input. Projections for SSP1 and SSP3 are developed in the same manner, using in addition scenario-specific assumptions on the convergence rates of educational variables to align the projections with the narratives of the two scenarios, as described in Section 3.3.

3.1. Bayesian Model Averaging (BMA)

We use the BMA method (Steel, 2020) to investigate the empirical drivers of changes in the proportion of the population within a specific age group with a particular level of educational attainment, and to create future projections. BMA is a technique of statistical inference that explicitly assesses model uncertainty by combining information from a multitude of individual models. In particular, in our application we consider all linear regression models that can be estimated by combining all available covariates. The outcome variable of interest is linearly regressed against each one of these combinations and the parameters of interest are obtained for each one of these specifications. BMA assigns weights to each one of these models, based on model fit (where the better fitting models receive a higher weight) and minimizing complexity (penalizing models with many explanatory variables). BMA creates a weighted average from the inference obtained by all of the models, resulting in a final prediction that considers all specifications but gives more importance to the more robust models (in terms of goodness of fit and simplicity). The use of particular prior distributions over the models entertained implies that some specifications can be excluded from the analysis or weighted down if they are deemed unsuitable. The constrains we imposed in the analysis for each age-sex-education category are outlined in the supplementary material (Tables S5, S6 and S7 in Supporting Information S1).

The method allows us to integrate specification uncertainty into the estimated effects of different covariates and in the projected trajectories. This type of uncertainty is related to the correct choice of models and specifications as well as which variables should be included in the specification. BMA accounts for such uncertainties by averaging over multiple model specifications, resulting in more robust estimates for the projections as opposed to relying on a single model. We consider regression specifications linking the share of persons in area i within a given age/education group (s_i) at a given year t to a set of explanatory variables contained in matrix x and measured at an initial period prior to year t. The class of models we entertain is thus given by linear regression specifications of the form

$$s_i = \alpha + \sum_{j=1}^{k} \beta_j x_{ji} + \varepsilon_{i,} \tag{1}$$

where k explanatory variables from a pool of K potential covariates are included in a particular model, α represents the intercept, β denotes the coefficients of the covariates, and ε_i the error term, assumed to fulfill the standard assumptions of the normal linear regression model. The uncertainty related to the choice of a group of covariates as regressors when carrying out inference about the effect of particular variables or computing projections can be integrated by constructing model weights. Assuming that we are interested in the quantity μ, which could be a parameter of the regression model or a prediction of the dependent variable, its posterior distribution is given by

$$P(\mu|\, y) = \sum_{m=1}^{2^K} P(\mu|\, y, M_m)\, P(M_m|\, y) \tag{2}$$

where $P(\mu \mid y)$ denotes the posterior distribution of the quantity, $P(\mu \mid y, M_m)$ is its posterior distribution under model M_m (defined by a particular choice of covariates) and $P(M_m \mid y)$ is the posterior model probability of model M_m. The posterior model probabilities of individual specifications are proportional to the product of the marginal likelihood of the model ($P(M_m \mid y)$) and its corresponding prior probability $P(M_m)$. In our application, we follow Fernandez et al. (2001) and Ley and Steel (2009) to implement the priors over parameters and over the inclusion of covariates.

In our application the set of covariates included in potential specifications consist of (a) the initial shares of populations classified by age, sex and education, (b) initial level of fertility, (c) initial level of mortality and (d)

23284277, 2024, 10, Downloaded from https://agupubs.onlinelibrary.wiley.com/doi/10.1029/2024EF004431 by Area Sistemi Dipart & Document, Wiley Online Library on [23/10/2024]. See the Terms and Conditions (https://onlinelibrary.wiley.com/terms-and-conditions) on Wiley Online Library for rules of use; OA articles are governed by the applicable Creative Commons License

initial level of internal migration flows. The population data used for this analysis, disaggregated by age, sex and education are available at census tract level from the Municipal Statistics Service in Madrid.

3.2. Data

Despite a growing number of epidemiological studies on heat-related excess mortality, only few studies assess the effect modification of vulnerability factors and those that do, employ fairly coarse resolutions, usually at a city-wide scale (e.g., Sera et al., 2019). In this article, we choose the determinants of vulnerability based on data availability at fine resolution matched with the type of data available in the SSP databases, namely demographic variables stratified by age, sex, education, mortality, fertility and internal migration. The selected variables have shown effect modification in epidemiological studies (Son et al., 2019).

Data from various sources were curated for input to the BMA framework. We obtain the population data from the Municipal Statistics Service in Madrid (Servicio Municipal de Estadística) for the year 2012, spanning information from 2409 census tracts, and for 2020, corresponding to 2,443 tracts. The population data are differentiated by sex (males and females), age group (25–64, 65–84 and 85+) and educational attainment (in three broad groups corresponding to a range between no-education (ISCED 0) and completed primary (ISCED 2) - low education, secondary (ISCED 3) - medium education and tertiary (ISCED 6 to 8) - high education). The categories for educational attainment have been translated from the Spanish education system to the International Standard Classification of Education (ISCED) by the authors (see supplementary Table S1 in Supporting Information S1 for details). Although infants (below one year of age) and young children (one to five years of age) are considered vulnerable to heat stress, our focus on educational attainment as a proxy for socioeconomic status and adaptive capacity leads to the exclusion of population below the age of 25 from our analysis. Mortality and fertility data from 1975 to 2019 at city-wide level and internal migration (population mobility between the 21 districts of Madrid) from 2019 were downscaled at census tract resolution to match the age-sex education data. We use population weights to recalculate the coarser data for mortality, fertility and internal migration at census tract resolution for men and women in three age groups: 25–64, 65–84 and 85+ and three education categories: low, medium and high. High-resolution (30 s) climate data from WorldClim (Fick & Hijmans, 2017) were combined with population data using coverage weighted means to geo-convert terrestrial grid cells of temperature to census tracts with boundaries defined by the national statistical agency. We used average maximum temperature in degrees Celsius for summer months (June-July-August) between 1970 and 2000. Supplementary Text S1 and S2 in Supporting Information S1 provide a more detailed description of the data collected and pre-processing. We apply our framework on the municipality of Madrid. The city is located at the center of the Iberian Peninsula at latitude 40°40′ North and longitude 3°70′ West, situated at an altitude of approximately 650 m. It has a municipal surface area of about 605 km^2 and 3.3 million inhabitants (Figure 2). According to the Köppen-Geiger climate classification (Beck et al., 2018), Madrid is characterized by Mediterranean climate (Csa) with hot summers, registering mean temperatures of 24–28°C (AEMET).

3.3. Projections in Alternative Scenarios

The projections of the education shares for each of the six age-sex groups are computed using model-averaged conditional predictions under assumptions that reproduce the narratives of three SSP scenarios: SSP1, SSP2 and SSP3. For projections based on the SSP2 scenario, we use model-averaged predictions of the specifications used under the assumption that internal migration flows remain constant at the level observed in our last in-sample observation (i.e., in 2019). For fertility and mortality dynamics, we apply the projected trends for Spain under this scenario (KC & Lutz, 2017) for all districts in Madrid, and the education shares are projected making use of the model-averaged parameters estimated with the sample at hand.

Projections for SSP1 and SSP3 are based on additional assumptions about the convergence patterns of education levels across the six age-sex groups, calculated using estimates of the slopes of the regression lines between changes in education levels between 2020 and 2050 and the corresponding educational level in 2020 for SSP1, SSP2, and SSP3 scenarios. The future convergence patterns of educational attainment are derived from global data covering 202 countries, obtained from the Wittgenstein Center data explorer platform. We estimated the convergence dynamics by regressing the global projected change in the corresponding shares between 2020 and 2050 against the shares in 2020 and evaluating the slope of the regression line *(m).* Values of *m* were first derived individually for each education category in all 202 countries for which data were available (six categories: no

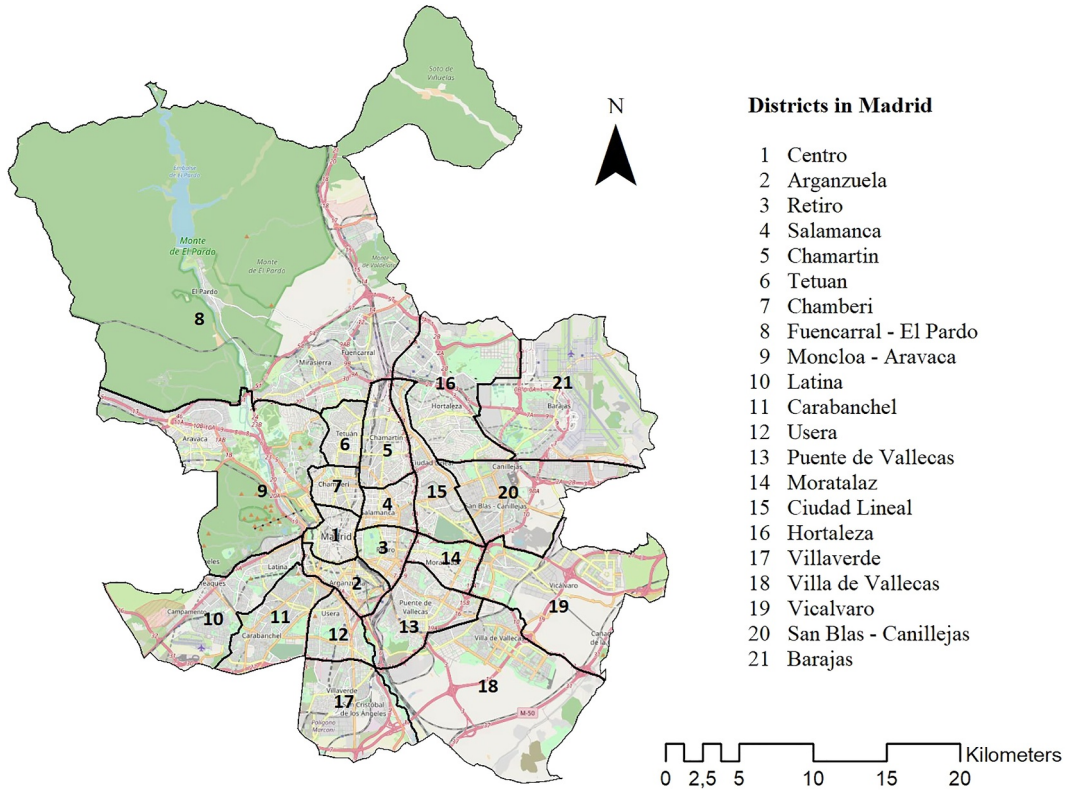

Figure 2. Municipality of Madrid, divided into its 21 districts. Base map source: Open Street Map.

education, incomplete, primary, lower secondary, upper secondary and post-secondary) and then averaged across the six education categories. The final values we obtained for the slopes are mSSP1 = −0.45, mSSP2 = −0.24 and mSSP3 = −0.03. We approximated the slope mSSP3 to zero, which implies that the ratio between mSSP3 and mSSP2 will also be zero, and the ratio between mSSP1 and mSSP2 was approximated at 2 (mSSP1/mSSP2 = 1.89).

The convergence speed allowed us to project the global trends of educational attainment, and impose them at any other spatial resolution, such as census tract resolution for Madrid in our case. Following the narratives corresponding to the SSP scenarios, the projections for SSP3 reveal that the convergence dynamics observed in the last decades across education shares will cease to exist in the coming years. For that purpose, we imposed a conditional convergence rate of zero across the census tracts of the city for each age, sex and education variables, and used the estimated effects of the other covariates obtained from the data. For the SSP1 scenario, we imposed an increased convergence rate of education in the projection period by 100% with respect to SSP2, based on the difference in estimates of the convergence speed across countries. Following this scenario-building strategy, the estimated trajectories have characteristics that quantitatively replicate the differences in convergence speed across countries implied by existing SSP projections (Crespo Cuaresma, 2017). A more detailed description of the computations can be found in the supplementary Text S5 in Supporting Information S1.

4. Results

4.1. Estimation of Current Vulnerability

We conducted the analysis in two steps. First, we investigated potential clusters of vulnerable areas using population data for Madrid that is stratified by age, sex and educational attainment at the census tract level for 2012 and 2020. Spatially interpolated monthly climate data for global land areas with a very high spatial resolution of 30 s (approximately 1 km^2), obtained from WorldClim (Fick & Hijmans, 2017) were used to approximate the

23284277, 2024, 10, Downloaded from https://agupubs.onlinelibrary.wiley.com/doi/10.1029/2024EF004431 by Area Sistemi Dipart & Document, Wiley Online Library on [23/10/2024]. See the Terms and Conditions (https://onlinelibrary.wiley.com/terms-and-conditions) on Wiley Online Library for rules of use; OA articles are governed by the applicable Creative Commons License

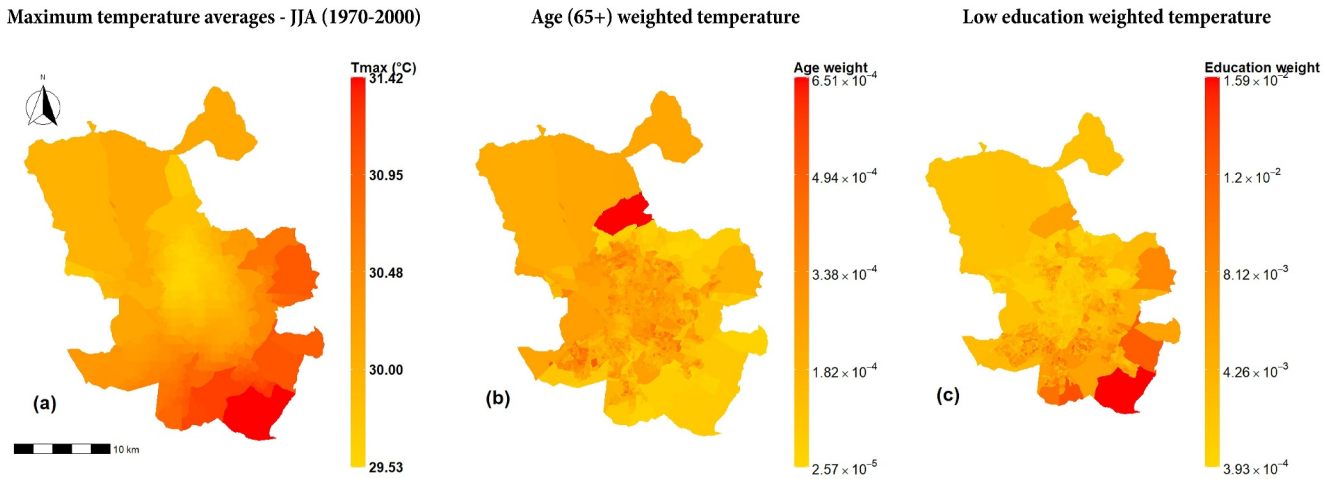

Figure 3. Population weighted temperatures in Madrid (1970–2000) at census tract resolution. Panel a exhibits the average maximum temperatures for June-July-August (JJA) between 1970 and 2000. Panels b and c combine the temperature data with information on population characteristics in each census tract to compute (b) the older population-weighted exposure in 2020 and (c) low-education-weighted exposure in 2020.

distribution of temperatures within Madrid in the past decades. We then combined these data with shares of population above 65 years and of population with low education to demonstrate how the distribution of heat stress changes depending on the vulnerability category used in the population-weighted computations. To achieve this, we performed spatial interpolation where we extracted and averaged the gridded temperature data within the boundaries of census tracts. We then computed simple population-weighted temperatures by multiplying temperature values with the 2020 shares of 65+ population (Figure 3b) and 2020 shares of population with low education (Figure 3c) and then normalizing by the total population in Madrid. Average maximum temperatures in summer months (June-July-August) between 1970 and 2000 show the highest temperatures in the south and east areas of Madrid (Figure 3a). We further analyzed the two most important vulnerability factors highlighted in the epidemiological literature, individually: heat stress population-weighted exposure of older adults, above 65 years (Romanello et al., 2021) (Figure 3b) and of groups with low socioeconomic status (Conte Keivabu 2022), using low educational attainment as a proxy (Figure 3c).

We find that the population in the central districts and northern parts of Madrid face higher heat stress due to their relatively older age. While central districts show a more even distribution of the population by age groups, east and south districts are dominated by younger populations (aged 25–64). El Goloso (shown in red in Figure 3b), located in the district of Fuencarral-El Pardo, exhibits the highest risk related to age, with approximately 73% of the population with 65 or more years of age, making this the oldest neighborhood in Madrid. In contrast, the south-eastern parts of the city face high risks of being unable to cope with heat, due to the relatively low socioeconomic status, reflected in the share of population with low educational attainment. District 18 - Villa de Vallecas is the district with the lowest educational attainment level in Madrid. With a total population of 114,512, more than 36.7% of its inhabitants have low educational attainment. The female population represents approximately 48.5% of the total population of the district, out of which 19.2% have a low level of education (17.5% is the corresponding share for men). The comparison between age and education weighted exposure (Figures 3b and 3c) reveals that the belt-shaped region immediately south of the city center faces a combined risk of heat stress due to aging of population and relatively low education levels.

4.2. Demographic Projections for Modeling Future Heat-Related Vulnerability

In the second step, we developed decadal, high resolution population projections between 2010 and 2050, for females and males of age groups 25–64, 65–84 and 85+ with low, medium and high education attainment (see supplementary Table S1 in Supporting Information S1 for the ISCED translation of the Spanish education system), for the scenarios corresponding to SSP1, SSP2 and SSP3 within the context of the demographic component of the SSPs.

23284277, 2024, 10, Downloaded from https://agupubs.onlinelibrary.wiley.com/doi/10.1029/2024EF004431 by Area Sistemi Dipart & Document, Wiley Online Library on [23/10/2024]. See the Terms and Conditions (https://onlinelibrary.wiley.com/terms-and-conditions) on Wiley Online Library for rules of use; OA articles are governed by the applicable Creative Commons License

10.1029/2024EF004431

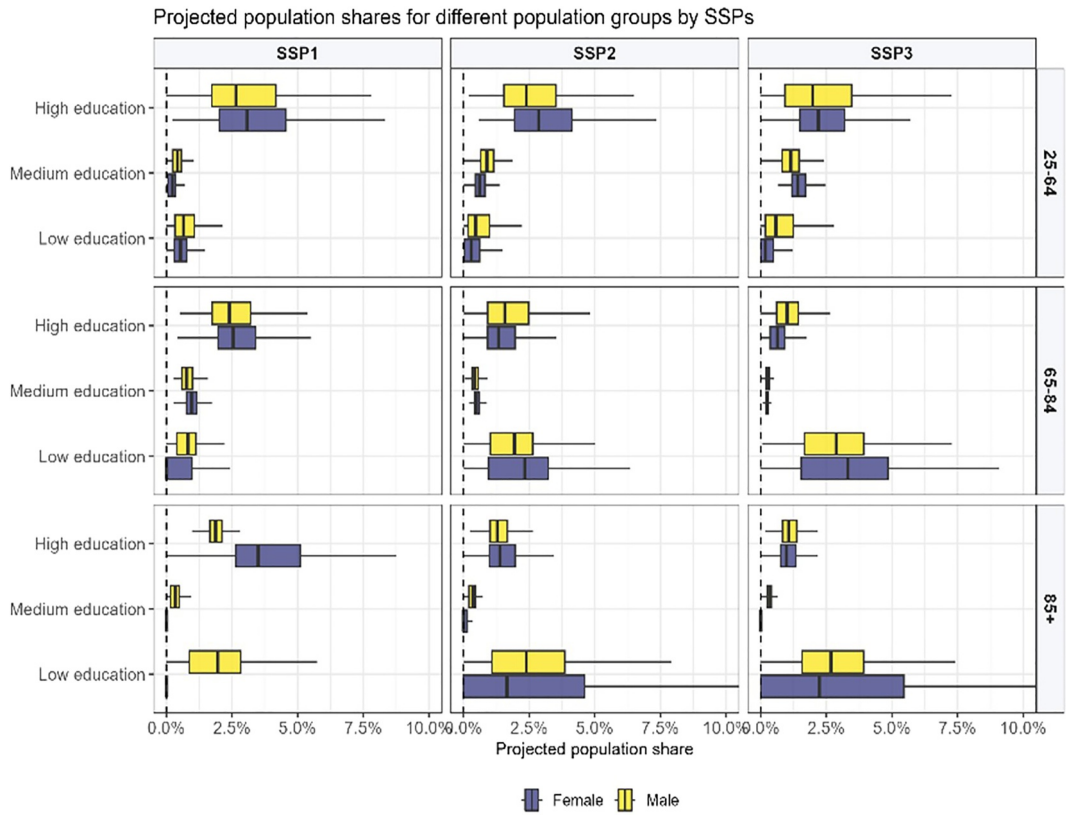

Figure 4. Projected population shares in 2050 for different population groups by SSPs. The population shares (*x*-axis) are shown distinguishing by sex and different education levels (high, medium, low) and age (25–64. 65–84, 85+) groups. The population shares across the different population groups sum to 100%. The boxplots show the distribution (median, interquartile ranges (IQR), and 1.5 × QR) of different model runs which form the basis of our projections using Bayesian Model Averaging.

The method was validated by comparing 2020 population projections for SSP2 with 2020 observed data at the same spatial resolution. Specifically, we performed a simple linear regression analysis between projected and observed population and assessed the correlations using R-squared values. The validation results show relatively high correlation between the projections and the observed data. For the low education group, we obtained R2: 0.71 (range 0.60–0.89), for medium, R2: 0.59 (range 0.36–0.76) and for high education R2: 0.80 (range 0.68–0.88) (see supplementary Table S4 in Supporting Information S1). We performed in-sample validation as the preferred out-of-sample validation was not possible due to lack of data at similar resolution from the previous decade (i.e., 2001).

4.2.1. Projections of City-Wide Trends

The analysis of the change in shares of the populations' educational attainment shows a general decrease in low and medium education and an increase in high education for all scenarios.

Figure 4 reflects the projected populations distribution in 2050 across the three age groups, differentiated by sex and educational attainment, along the three SSP scenarios. SSP1 projections show an increase in the share of populations with high education, especially for women. The share of males above 85 years register the smallest increase in high education and a similar increase in the share of low education, although the interquartile range is wider for the latter, suggesting a larger uncertainty. Similarly, SSP2 projections display a slightly smaller but consistent increase in the share of populations with high education for the 25–64 age group. The increase in shares of older adults (65–84 and 85+) is however smaller. These age groups also show an increase in shares of low education. Females above the age of 85 years show the strongest increase in low education. As expected, SSP3

23284277, 2024, 10, Downloaded from https://agupubs.onlinelibrary.wiley.com/doi/10.1029/2024EF004431 by Area Sistemi Dipart & Document, Wiley Online Library on [23/10/2024]. See the Terms and Conditions (https://onlinelibrary.wiley.com/terms-and-conditions) on Wiley Online Library for rules of use; OA articles are governed by the applicable Creative Commons License

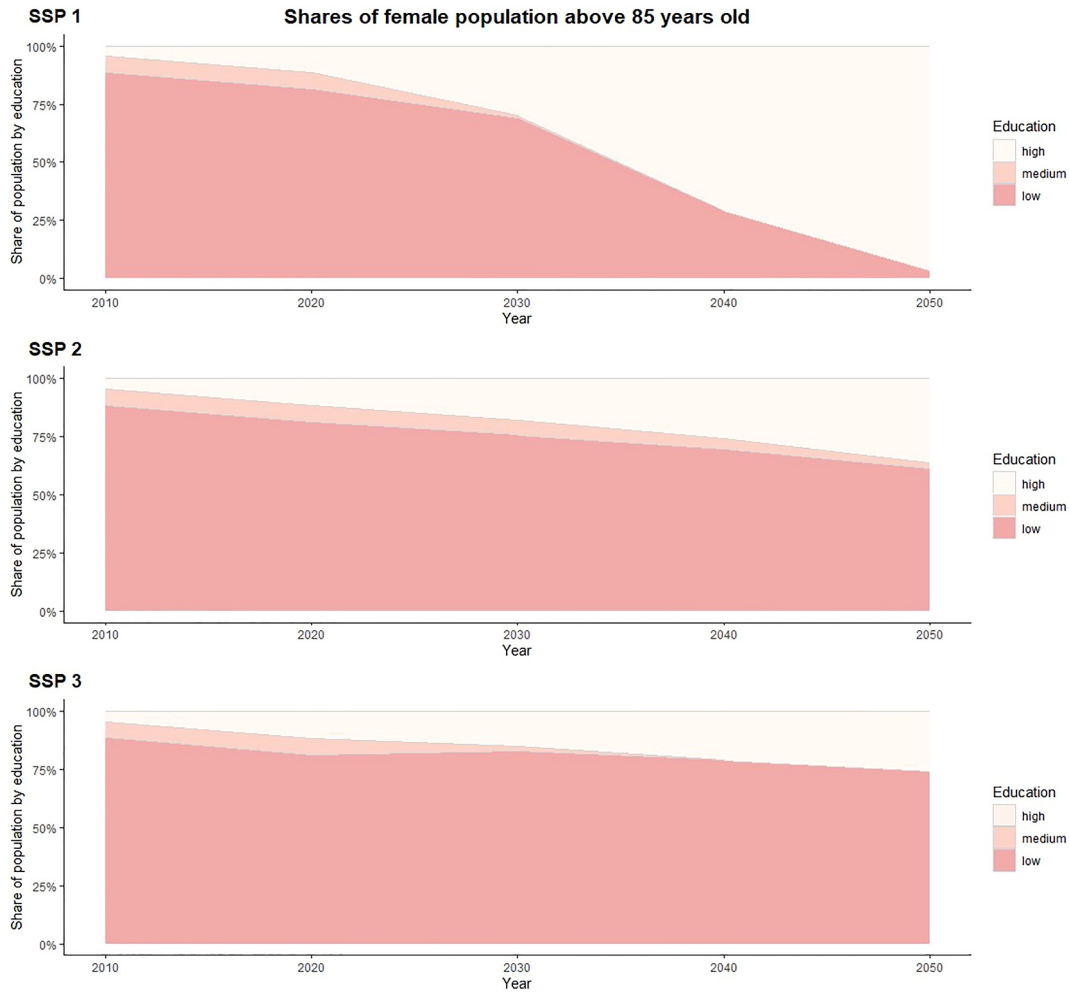

Figure 5. Changes in education share of females above 85 years. Change over time between 2012 and 2050 in the shares of low, medium and high educated women for SSP1 (top panel), SSP2 (middle panel) and SSP3 (bottom panel).

projections register the smallest increase of shares of high education and the largest increase in shares of low education across all age and sex groups. Young women aged 25 to 64 register the largest increase in high education category while males aged 65 to 84 show the smallest increase in shares of high education.

The projections are computed for each age and sex group separately and normalized to 100% per age-sex group. Figure 5 shows changes in average education levels among women aged 85 and older in Madrid, under three different scenarios. In the SSP1 scenario (top panel in Figure 5), the percentage of women aged 85 and above with only primary and secondary education decreases sharply, reaching values close to zero in 2050. This decline is compensated by the corresponding rise in the percentage of women with tertiary education, in the same age group. The sharpest decrease takes place between 2030 and 2040, suggesting that in the SSP1 narrative, older adults are inclined to get higher education later in life if they did not do so during their youth. The SSP2 scenario (middle panel in Figure 5) depicts a gradual and consistent decline in the proportion of women with lower levels of education. The medium education category shows very little variation, while highly educated population increases gradually over time. SSP3 projections (bottom panel in Figure 5) show a small increase in the proportion of women aged 85 and above with low education toward 2030, followed by a slight decrease thereafter. Similar to SSP2, the medium education category shows little to no variation and high education shows a slight increase throughout the first half of the century.

23284277, 2024, 10, Downloaded from https://agupubs.onlinelibrary.wiley.com/doi/10.1029/2024EF004431 by Area Sistemi Dipart & Document, Wiley Online Library on [23/10/2024]. See the Terms and Conditions (https://onlinelibrary.wiley.com/terms-and-conditions) on Wiley Online Library for rules of use; OA articles are governed by the applicable Creative Commons License

10.1029/2024EF004431

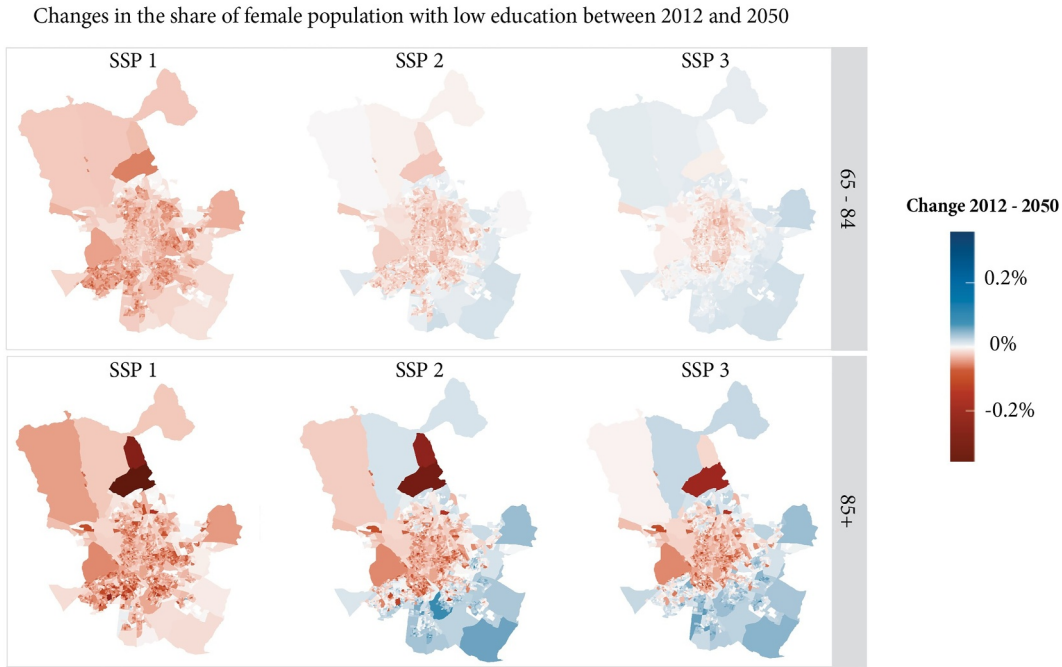

Figure 6. Projected changes in the spatial distribution of vulnerable groups until 2050. The panels show changes in the female population aged 65 to 84 and above 85 years with low education for SSP1, SSP2 and SSP3. Decrease in shares of low education is shown in red and increase is shown in blue.

4.2.2. Spatial Distribution of Vulnerability at High Spatial Resolution

The spatial distribution of educational attainment varies substantially across the three scenarios. The proportion of low educated in the younger age group (men and women aged between 25 and 64 years) decreases in most areas toward 2050. There are a few exceptions from this trend however. Neighborhoods such as El Goloso, show a slight increase in low education shares for both young men and women in all three scenarios. Areas that show this type of dynamic are typically characterized by large shares of older populations and potentially by emigration of young and highly educated individuals. Conversely, districts in the south-eastern parts of Madrid, which are predominantly younger populations, show the strongest decrease in shares of low education in all three scenarios (see all results in supplementary Figures S1, S2 and S3 in Supporting Information S1). Older age groups exhibit greater disparities in education-related vulnerability for both men and women. The age Group 65 to 84 shows a general decrease in low education shares in SSP1, with the decline being more pronounced for women in most areas. While for males there is even a small increase in a few census tracts in the eastern districts. Similarly, a reduction in the proportion of individuals with low levels of education is observed in most census tracts under SSP2. Notably, the magnitude of this decline is more pronounced for women than for men. However, in certain areas in the west, there is even a decline in population of low educated females and an increase in the population of low educated males.

SSP3 projections also show a positive change in the shares of population with low level of education for both sexes, meaning that several districts in the south and east would see an increase in the share of least educated population groups under this scenario. Projections for the age group 65 to 84 under SSP3 show an increase in the proportion of population with low level of education in most census tracts, with a slightly higher magnitude for women. Central districts show a decline in the proportion of population with low levels of education, the decline being more pronounced for women. The magnitude of negative change in the central districts is substantial for both males and females, resulting in an overall negative value. This suggests a large gap between the "highly educated" and "low educated" within this age group in SSP3.

Figure 6 illustrates changes in the proportion of older women for 65–84 and 85+ age groups with lowest educational attainment between 2012 and 2050. Projections for all other age-sex groups are included in

23284277, 2024, 10, Downloaded from https://agupubs.onlinelibrary.wiley.com/doi/10.1029/2024EF004431 by Area Sistemi Dipart & Document, Wiley Online Library on [23/10/2024]. See the Terms and Conditions (https://onlinelibrary.wiley.com/terms-and-conditions) on Wiley Online Library for rules of use; OA articles are governed by the applicable Creative Commons License

23284277, 2024, 10, Downloaded from https://agupubs.onlinelibrary.wiley.com/doi/10.1029/2024EF004431 by Area Sistemi Dipart & Document, Wiley Online Library on [23/10/2024]. See the Terms and Conditions (https://onlinelibrary.wiley.com/terms-and-conditions) on Wiley Online Library for rules of use; OA articles are governed by the applicable Creative Commons License

supplementary Figures S7, S8 and S9 in Supporting Information S1. Under SSP1, a decline in the proportion of these two particularly vulnerable groups is consistent and apparent across all districts. In this scenario, there is a noteworthy improvement in the educational attainment for older females and nearly all areas in Madrid experience a reduction in the proportion of individuals with low educational attainment. The strongest decline is projected to occur in the central districts and the slowest decline in the southern districts. Under SSP2, several districts in the south and east are projected to witness an increase in the population of the least educated females in both age groups. This implies these areas could be particularly vulnerable to heat stress if the current trends of population dynamics persist. In contrast to the projections under SSP1 and SSP2, SSP3 projections show an overall increase in vulnerability related to educational attainment in the majority of districts except for some central districts that are presently considered the wealthier areas of Madrid. This suggests an important disparity between the affluent and the disadvantaged in this scenario. The magnitude of change, both positive and negative, appears more pronounced in the older age group, those aged 85 and above.

5. Discussion and Conclusions

Vulnerability to heat stress can be quantified by demographic variables describing population subgroups, including older adults, women and individuals with low socioeconomic status. Vulnerability varies substantially in space, within intra-urban areas and over time. Preserving demographic heterogeneity, stratified by population subgroups in high-resolution projections is essential for conducting urban risk assessments and adaptation planning in the context of a warming climate. In this article, we address the need for granular vulnerability modeling. We estimated demographic trends extracted from global population data and applied them to the very high resolution data in Madrid to create spatially explicit and demographically heterogeneous local projections of the SSP scenarios.

The convergence approach used to project our population variables is inspired by the methods in Crespo Cuaresma (2017) and used to quantify the scenario trajectories described by the SSP narratives. We combined regression-based projections obtained using BMA with global convergence speed estimates of educational attainment within three of the five SSPs. We then applied these convergence speeds across six different age-sex categories to generate very high-resolution projections of vulnerability to heat stress, that are consistent with the narratives of these three scenarios. Incorporating population projections within a vulnerability modeling framework provides an ideal opportunity to examine the interplay between population dynamics and climate risk. Our analysis shows how following a sustainable trajectory (SSP1) is expected to decrease vulnerability to heat stress in the future, whereas a development that follows current trends (SSP2) or a conflict dominated scenario (SSP3) widens the existing gap between privileged and deprived neighborhoods, even in the capital city of a rich OECD country like Spain.

The average vulnerability differences among the three scenarios are primarily driven by the changes in age and education distribution. Overall vulnerability in Madrid is projected to decrease gradually and consistently over time in all three scenarios, including SSP3. However, preserving the demographic heterogeneity in the projections implies that convergence dynamics will produce distinct effects across the different age-sex groups within the same scenario. This effect is particularly noticeable when comparing the SSP3 projections for women. In the 25 to 64 age group, the proportion of women with low level of education decreases consistently in almost all regions of the city, but education-related vulnerability increases substantially in the older age groups. Furthermore, spatial dynamics play a key role, showing older women with higher level of education concentrating in the central districts - the wealthier parts of the city also today - leaving the peripheral areas increasingly more vulnerable. The fragmentation narrative that dominates SSP3 becomes strikingly evident across the age-sex groups as well as across neighborhoods with different levels of wealth in Madrid. Conversely, the sharp decrease in inequality in SSP1 drives the population dynamics toward a more uniform and resilient change, with the exception being males in the 85+ age group (see supplementary Figure S9 in Supporting Information S1). These patterns show that vulnerability is highly complex and dynamic, consisting of a multitude of factors which interact and form a reinforcing feedback loop, leading either toward fragmentation or resilience.

The application of BMA based projections in this paper presents a framework for mapping heat vulnerability clusters at the intra-urban level and for projecting potential future changes under three scenarios aligned with the SSPs. This allows for addressing existing challenges in planning and implementation of adaptation measures. This research framework is also applicable to other locations and at different scales. Nonetheless, the results are

23284277, 2024, 10, Downloaded from https://agupubs.onlinelibrary.wiley.com/doi/10.1029/2024EF004431 by Area Sistemi Dipart & Document, Wiley Online Library on [23/10/2024]. See the Terms and Conditions (https://onlinelibrary.wiley.com/terms-and-conditions) on Wiley Online Library for rules of use; OA articles are governed by the applicable Creative Commons License

most useful at the highest resolution for which input data are available—preferably at the census tract level, enabling policy making to account for the unique characteristics of different areas within the city. Primarily focusing on vulnerability quantification based on demographic variables, our approach serves as a key first step in informing local adaptation planning and opening opportunities for further research to expand on this framework by incorporating different other factors underlying vulnerability. These could include elements of urban planning, such as proximity to green (e.g., parks) and blue (e.g., fountains) spaces, public health characteristics, such as populations' history of cardiopulmonary diseases as well as economic factors such as GDP per capita and income. As global warming trends will persist across all future scenarios, further research is needed to identify the most effective adaptation solutions. These may encompass initiatives such as cooling centers and personalized home visits, designed to meet the specific needs of these vulnerable communities.

Our study faces different limitations which are important for the interpretation of our findings. One limitation is that we restrict our projections to demographic variables (due to data availability), although vulnerability is admittedly a more complex phenomenon. Socioeconomic characteristics, urban planning features and behavioral aspects play an important role in how vulnerability is shaped and how it changes within a city. Vulnerability scenarios should ideally encompass all of these factors, but scenarios require methods that account for specific local trends as well as means of coupling with global changes. Scenario data, as well as raw data at resolutions that are relevant for local decision makers are limited and therefore high-resolution scenario development is, for now at least, restricted to those characteristics for which data are available both in the SSPs and locally.

Another limitation pertains to potential changes in migration both within and beyond Madrid, which may vary by the SSPs. While our approach accounts for internal migration between the city's districts, we have not modelled differences in future mobility patterns under the different socioeconomic scenarios considered. In addition, international migration or narratives related to potential changes in migration to other regions of Spain have not been explicitly taken into account. These forms of mobility can be important if, for example, vulnerable population groups move to areas less affected by heat stress. Our projection framework allows for the integration of different migration scenarios by extending the set of assumptions used. Given that no accurate projections on differential migration patterns by SSPs are available for the Spanish context, we have not incorporated such variations in the migration variables into our current modelling framework.

Finally, climate and risk literature outlines a wide variety of metrics and indices for measuring heat-related climate risks and vulnerability. However, very few of these metrics are developed based on their direct, measured impacts on health outcomes such as mortality. Most existing indices rely on hazard indicators or socioeconomic characteristics but not the interaction between them. While useful for mapping potential risks, such approaches may not accurately reflect the true health impacts. This is also a limitation of our research. An assessment of the influence of various vulnerability factors would require a detailed epidemiological analysis at the census tract level to accurately correlate specific factors with health outcomes like mortality, which is beyond the scope of our study.

Data Availability Statement

All data used in this analysis are publicly available. Demographic data at census tract resolution was obtained via email correspondence with the Municipal Statistical Office (Estadística—Ayuntamiento de Madrid, 2024, www.madrid.es/estadistica). The census tract shapefiles used for the figures are available at: MADRID, INSTITUTO DEESTADíSTICA DE LA COMUNIDAD DE (2024, https://gestiona.comunidad.madrid/nomecalles/Inicio.icm). The historical climate data is available at: https://www.worldclim.org/data/worldclim21.html. Global projections of population by age, sex and educational attainment at the country level for the three SSPs can be obtained from (Wittgenstein Centre Human Capital Data Explorer, 2018) and the Wittgenstein Center Data Explorer: https://dataexplorer.wittgensteincentre.org/wcde-v2/. For a detailed description of the data sources and data preprocessing, see Supplementary Text S1 and S2 in Supporting Information S1. The datasets generated and analyzed during the study as well as replication *R* code and the full dataset required to reproduce the results are available in Marginean (2024) and on the GitHub repository: Iulia Marginean GitHub (2023, https://github.com/IuliaMargineanGitHub/Projecting-Heat-Stress-Vulnerable-Populations-at-Intra-Urban-Scales).

Acknowledgments
The authors would like to thank Paloma Yanez for liaising with and gathering data from the Municipal Statistics Service in Madrid; to Nina Schuhen for advising on approaches to integrate the raw datasets on age and education and not last, to Eilif Ursin Reed for the stylizing Figure 1 of the manuscript. This research is part of the EmCliC project: Embodying Climate Change: Transdisciplinary Research on Urban Overheating—www.emclic.com. The project is funded from the EEA grants 2014–2021 under the Basic Research Programme operated by the Polish National Science Centre in cooperation with the Research Council of Norway (Grant 2019/35/J/HS6/03992). Jesus Crespo Cuaresma acknowledges support from the eXplore! initiative, funded by the B&C Privatstiftung and Michael Tojner. ChatGPT, version 4 was used in the final editing and English proofing of some sections of this manuscript.

References

Achebak, H., Devolder, D., & Ballester, J. (2019). Trends in temperature-related age-specific and sex-specific mortality from cardiovascular diseases in Spain: A national time-series analysis. *The Lancet Planetary Health*, *3*(7), e297–e306. https://doi.org/10.1016/S2542-5196(19)30090-7

Åström, O., Bertil, F., Bertil, F., & Joacim, R. (2011). Heat wave impact on morbidity and mortality in the elderly population: A review of recent studies. *Maturitas*, *69*(2), 99–105. https://doi.org/10.1016/j.maturitas.2011.03.008

Basu, R. (2009). High ambient temperature and mortality: A review of epidemiologic studies from 2001 to 2008. *Environmental Health*, *8*(1), 40. https://doi.org/10.1186/1476-069X-8-40

Beck, H. E., Zimmermann, N. E., McVicar, T. R., Vergopolan, N., Berg, A., & Wood, E. F. (2018). Present and future köppen-geiger climate classification maps at 1-km resolution. *Scientific Data*, *5*(1), 180214. https://doi.org/10.1038/sdata.2018.214

Begum, R. A., Lempert, R. J., Ali, E., Benjaminsen, T. A., Bernauer, T., Cui, X., et al. (2022). Points of departure and key concepts. *Climate Change 2022: Impacts, Adaptation and Vulnerability. Contribution of Working Group II to the Sixth Assessment Report of the Intergovernmental Panel on Climate Change*, 121–196. https://doi.org/10.1017/9781009325844.003

Benmarhnia, T., Deguen, S., Kaufman, J. S., & Smargiassi, A. (2015). Review article: Vulnerability to heat-related mortality. *Epidemiology*, *26*(6), 781–793. https://doi.org/10.1097/EDE.0000000000000375

Birkmann, J., Sauter, H., Garschagen, M., Fleischhauer, M., Puntub, W., Klose, C., et al. (2021). New methods for local vulnerability scenarios to heat stress to inform urban planning—Case study city of ludwigsburg/Germany. *Climatic Change*, *165*(1), 37. https://doi.org/10.1007/s10584-021-03005-3

Butz, W. P., Lutz, W., & Sendzimir, J. (2014). Education and differential vulnerability to natural disasters. Reprint from Ecology and Society. Vienna, Austria. *International Institute for Applied Systems Analysis*.

Calleja-Agius, J., England, K., & Calleja, N. (2021). The effect of global warming on mortality. *Early Human Development*, *155*(April), 105222. https://doi.org/10.1016/j.earlhumdev.2020.105222

Chong, A., & Martinez, J. (2021). Does education increase risk aversion in households? Some evidence using artefactual experiments in Peru. *Latin American Economic Review*, *30*(September), 1–19. https://doi.org/10.47872/laer.v30.22

Cissé, G., McLeman, R., Adams, H., Aldunce, P., Bowen, K., Campbell-Lendrum, D., et al. (2022). Health, wellbeing and the changing structure of communities. In H.-O. Pörtner, D. C. Roberts, M. M. B. Tignor, E. S. Poloczanska, K. Mintenbeck, A. Alegría, et al (Eds.), *Climate change 2022: Impacts, adaptation and vulnerability. Contribution of working group II to the sixth assessment report of the intergovernmental panel on climate change*. Cambridge University Press.

Conlon, K. C., Mallen, E., Gronlund, C. J., Berrocal, V. J., Larsen, L., & O'Neill, M. S. (2020). Mapping human vulnerability to extreme heat: A critical assessment of heat vulnerability indices created using principal components analysis. *Environmental Health Perspectives*, *128*(9), 097001. https://doi.org/10.1289/EHP4030

Conte Keivabu, R. (2022). Extreme temperature and mortality by educational attainment in Spain, 2012–2018. *European Journal of Population*, *38*(5), 1145–1182. https://doi.org/10.1007/s10680-022-09641-4

Copernicus Climate Change Service (2019). Climate variables for cities in europe from 2008 to 2017. [Object]. https://doi.org/10.24381/CDS.C6459D3A

CORDEX Regional Climate Model Data on Single Levels (2019). CORDEX regional climate model data on single levels. [Object]. https://doi.org/10.24381/CDS.BC91EDC3

Crespo Cuaresma, J. (2017). Income projections for climate change research: A framework based on human capital dynamics. *Global Environmental Change*, *42*(January), 226–236. https://doi.org/10.1016/j.gloenvcha.2015.02.012

Davidson, C., Lee Shing, Y., McKay, C., Rafetseder, E., & Wijeakumar, S. (2023). The first year in formal schooling improves working memory and academic abilities. *Developmental Cognitive Neuroscience*, *60*(April), 101205. https://doi.org/10.1016/j.dcn.2023.101205

Dimitrova, A., & Muttarak, R. (2020). After the floods: Differential impacts of rainfall anomalies on child stunting in India. *Global Environmental Change*, *64*(September), 102130. https://doi.org/10.1016/j.gloenvcha.2020.102130

Ebi, K. L., Hasegawa, T., Hayes, K., Monaghan, A., Paz, S., & Berry, P. (2018). Health risks of warming of 1.5°C, 2°C, and higher, above pre-industrial temperatures. *Environmental Research Letters*, *13*(6), 063007. https://doi.org/10.1088/1748-9326/aac4bd

Estadística—Ayuntamiento de Madrid. (2024). Retrieved from https://www.madrid.es/portales/munimadrid/es/Inicio/El-Ayuntamiento/Estadistica?vgnextchannel=8156e39873674210VgnVCM1000000b205a0aRCRD

Fernandez, C., Ley, E., & Steel, M. (2001). Model uncertainty in cross-country growth regressions. *Econometrics*, *16*(5), 563–576. University Library of Munich, Germany. https://doi.org/10.1002/jae.623

Fick, S. E., & Hijmans, R. J. (2017). WorldClim 2: New 1-km spatial resolution climate surfaces for global land areas. *International Journal of Climatology*, *37*(12), 4302–4315. https://doi.org/10.1002/joc.5086

Gao, J. (2017). Downscaling global spatial population projections from 1/8-degree to 1-km grid cells. *NCAR Library*. https://doi.org/10.5065/D60Z721H

Garschagen, M., Doshi, D., Moure, M., James, H., & Shekhar, H. (2021). The consideration of future risk trends in national adaptation planning: Conceptual gaps and empirical lessons. *Climate Risk Management*, *34*(January), 100357. https://doi.org/10.1016/j.crm.2021.100357

Gasparrini, A., Guo, Y., Hashizume, M., Lavigne, E., Zanobetti, A., Schwartz, J., et al. (2015). Mortality risk attributable to high and low ambient temperature: A multicountry observational study. *The Lancet*, *386*(9991), 369–375. https://doi.org/10.1016/S0140-6736(14)62114-0

Gasparrini, A., Guo, Y., Sera, F., Vicedo-Cabrera, A. M., Huber, V., Tong, S., et al. (2017). Projections of temperature-related excess mortality under climate change scenarios. *The Lancet Planetary Health*, *1*(9), e360–e367. https://doi.org/10.1016/S2542-5196(17)30156-0

Haines, A., & Ebi, K. (2019). The imperative for climate action to protect health. *New England Journal of Medicine*, *380*(3), 263–273. https://doi.org/10.1056/NEJMra1807873

Hauer, M. E. (2019). Population projections for U.S. Counties by age, sex, and race controlled to shared socioeconomic pathway. *Scientific Data*, *6*(February), 190005. https://doi.org/10.1038/sdata.2019.5

Hoffmann, R., & Muttarak, R. (2017). Learn from the past, prepare for the future: Impacts of education and experience on disaster preparedness in the Philippines and Thailand. *World Development*, *96*(August), 32–51. https://doi.org/10.1016/j.worlddev.2017.02.016

Honda, Y., Kondo, M., McGregor, G., Kim, H., Guo, Y. L., Hijioka, Y., et al. (2014). Heat-related mortality risk model for climate change impact projection. *Environmental Health and Preventive Medicine*, *19*(1), 56–63. https://doi.org/10.1007/s12199-013-0354-6

Hsu, A., Sheriff, G., Chakraborty, T., & Diego, M. (2021). Disproportionate exposure to urban heat island intensity across major US cities. *Nature Communications*, *12*(1), 2721. https://doi.org/10.1038/s41467-021-22799-5

Iulia Marginean GitHub. (2023). IuliaMargineanGitHub/Projecting-Heat-Stress-Vulnerable-Populations-at-Intra-Urban-Scales. Retrieved from https://github.com/IuliaMargineanGitHub/Projecting-Heat-Stress-Vulnerable-Populations-at-Intra-Urban-Scales

23284277, 2024, 10, Downloaded from https://agupubs.onlinelibrary.wiley.com/doi/10.1029/2024EF004431 by Area Sistemi Dipart & Document, Wiley Online Library on [23/10/2024]. See the Terms and Conditions (https://onlinelibrary.wiley.com/terms-and-conditions) on Wiley Online Library for rules of use; OA articles are governed by the applicable Creative Commons License

Jay, O., Capon, A., Berry, P., Broderick, C., De Dear, R., George, H., et al. (2021). Reducing the health effects of hot weather and heat extremes: From personal cooling strategies to green cities. *The Lancet*, *398*(10301), 709–724. https://doi.org/10.1016/S0140-6736(21)01209-5

Jiang, L., & O'Neill, B. C. (2017). Global urbanization projections for the shared socioeconomic pathways. *Global Environmental Change*, *42*(January), 193–199. https://doi.org/10.1016/j.gloenvcha.2015.03.008

Jones, B., O'Neill, B. C., & Gao, J. (2020). *Global one-eighth degree population base year and projection grids for the shared socioeconomic pathways (SSPs), revision 01*. NASA Socioeconomic Data and Applications Center (SEDAC). https://doi.org/10.7927/M30P-J498

Jurgilevich, A., Räsänen, A., Groundstroem, F., & Juhola, S. (2017). A systematic review of dynamics in climate risk and vulnerability assessments. *Environmental Research Letters*, *12*(1), 013002. https://doi.org/10.1088/1748-9326/aa5508

Kc, S., & Lutz, W. (2017). The human core of the shared socioeconomic pathways: Population scenarios by age, sex and level of education for all countries to 2100. *Global Environmental Change*, *42*, 181–192. https://doi.org/10.1016/j.gloenvcha.2014.06.004

Ley, E., & Steel, M. F. J. (2009). On the effect of prior assumptions in bayesian model averaging with applications to growth regression. *Journal of Applied Econometrics*, *24*(4), 651–674. https://doi.org/10.1002/jae.1057

Liu, Z., Anderson, B., Yan, K., Dong, W., Liao, H., & Shi, P. (2017). Global and regional changes in exposure to extreme heat and the relative contributions of climate and population change. *Scientific Reports*, *7*(1), 43909. https://doi.org/10.1038/srep43909

Lloyd, S. J., Quijal-Zamorano, M., Achebak, H., Hajat, S., Muttarak, R., Striessnig, E., & Ballester, J. (2023). The direct and indirect influences of interrelated regional-level sociodemographic factors on heat-attributable mortality in europe: Insights for adaptation strategies. *Environmental Health Perspectives*, *131*(8), 087013. https://doi.org/10.1289/EHP11766

López-Bueno, J. A., Díaz, J., Sánchez-Guevara, C., Sánchez-Martínez, G., Franco, M., Gullón, P., et al. (2020). The impact of heat waves on daily mortality in districts in Madrid: The effect of sociodemographic factors. *Environmental Research*, *190*(November), 109993. https://doi.org/10.1016/j.envres.2020.109993

Lutz, W., Muttarak, R., & Striessnig, E. (2014). Universal education is key to enhanced climate adaptation. *Science*, *346*(6213), 1061–1062. https://doi.org/10.1126/science.12579

MADRID, INSTITUTO DEESTADíSTICA DE LA COMUNIDAD DE. (2024). Nomecalles. Retrieved from https://gestiona.comunidad.madrid/nomecalles/Inicio.icm

Marginean, I. (2024). Iuliamargineangithub/projecting-heat-stress-vulnerable-populations-at-intra-urban-scales: Projecting heat stress vulnerable populations at intra-urban scales June 19, 2024 Release (Version 1.1.0). *Zenodo*. [Dataset]. https://doi.org/10.5281/zenodo.12165386

Min, J. Y., Lee, H.-S., Choi, Y.-S., & Min, K. (2021). Association between income levels and prevalence of heat- and cold-related illnesses in Korean adults. *BMC Public Health*, *21*(1), 1264. https://doi.org/10.1186/s12889-021-11227-4

Muttarak, R. (2021). Demographic perspectives in research on global environmental change. *Population Studies*, *75*(sup1), 77–104. https://doi.org/10.1080/00324728.2021.1988684

Muttarak, R., & Lutz, W. (2014). Is education a key to reducing vulnerability to natural disasters and hence unavoidable climate change? *Ecology and Society*, *19*(1), art42. https://doi.org/10.5751/es-06476-190142

O'Neill, B., van Aalst, M., Ibrahim, Z. Z., Ford, L. B., Bhadwal, S., Buhaug, H., et al. (2022). Key risks across sectors and regions. In H.-O. Pörtner, D. C. Roberts, M. M. B. Tignor, E. S. Poloczanska, K. Mintenbeck, A. Alegría, et al (Eds.), *Climate change 2022: Impacts, adaptation and vulnerability. Contribution of working group II to the sixth assessment report of the intergovernmental panel on climate change*. Cambridge University Press.

O'Neill, B. C., Kriegler, E., Ebi, K. L., Kemp-Benedict, E., Riahi, K., Rothman, D. S., et al. (2017). The roads ahead: Narratives for shared socioeconomic pathways describing world futures in the 21st century. *Global Environmental Change*, *42*(January), 169–180. https://doi.org/10.1016/j.gloenvcha.2015.01.004

Osberghaus, D., & Thomas, A. (2022). Heat vulnerability and adaptation of low-income households in Germany. *Global Environmental Change*, *72*(January), 102446. https://doi.org/10.1016/j.gloenvcha.2021.102446

Piel, F. B., Fecht, D., Hodgson, S., Blangiardo, M., Toledano, M., Hansell, A. L., & Paul, E. (2020). Small-area methods for investigation of environment and health. *International Journal of Epidemiology*, *49*(2), 686–699. https://doi.org/10.1093/ije/dyaa006

Puga-Gonzalez, I., Bacon, R. J., Voas, D., LeRon Shults, F., George, H., & Wildman, W. J. (2022). Adapting cohort-component methods to a microsimulation: A case study. *Social Science Computer Review*, *40*(4), 1054–1068. https://doi.org/10.1177/08944393221082685

Riahi, K., Van Vuuren, D. P., Kriegler, E., Edmonds, J., O'Neill, B. C., Fujimori, S., et al. (2017). The shared socioeconomic pathways and their energy, land use, and greenhouse gas emissions implications: An overview. *Global Environmental Change*, *42*(January), 153–168. https://doi.org/10.1016/j.gloenvcha.2016.05.009

Rohat, G., Flacke, J., Dosio, A., Pedde, S., Dao, H., & Van Maarseveen, M. (2019). Influence of changes in socioeconomic and climatic conditions on future heat-related health challenges in europe. *Global and Planetary Change*, *172*, 45–59. https://doi.org/10.1016/j.gloplacha.2018.09.013

Romanello, M., McGushin, A., Di Napoli, C., Drummond, P., Hughes, N., Jamart, L., et al. (2021). The 2021 report of the lancet countdown on health and climate change: Code red for a healthy future. *The Lancet*, *398*(10311), 1619–1662. https://doi.org/10.1016/S0140-6736(21)01787-6

Schneider, A., Zhang, S., Rai, M., Breitner, S., Stafoggia, M., De' Donato, F., et al. (2022). Effects of air temperature modified by vulnerability factors. *Zenodo*. https://doi.org/10.5281/ZENODO.7308761

Sera, F., Armstrong, B., Tobias, A., Vicedo-Cabrera, A. M., Åström, C., Bell, M. L., et al. (2019). How urban characteristics affect vulnerability to heat and cold: A multi-country analysis. *International Journal of Epidemiology*, *48*(4), 1101–1112. https://doi.org/10.1093/ije/dyz008

Smargiassi, A., Goldberg, M. S., Plante, C., Fournier, M., Baudouin, Y., & Kosatsky, T. (2009). Variation of daily warm season mortality as a function of micro-urban heat islands. *Journal of Epidemiology and Community Health*, *63*(8), 659–664. https://doi.org/10.1136/jech.2008.078147

Smid, M., & Costa, A. C. (2018). Climate projections and downscaling techniques: A discussion for impact studies in urban systems. *International Journal on the Unity of the Sciences*, *22*(3), 277–307. https://doi.org/10.1080/12265934.2017.1409132

Son, J. Y., Jia, C. L., & Bell, M. L. (2019). Temperature-related mortality: A systematic review and investigation of effect modifiers. *Environmental Research Letters*, *14*(7), 073004. https://doi.org/10.1088/1748-9326/ab1cdb

Stafoggia, M., Schneider, A., Rai, M., Zhang, S., Breitner, S., Gasparrini, A., et al. (2021). Effects of air temperature on cardiopulmonary mortality and morbidity in europe. *Zenodo*. https://doi.org/10.5281/ZENODO.5742457

Steel, M. F. J. (2020). Model averaging and its use in economics. *Journal of Economic Literature*, *58*(3), 644–719. https://doi.org/10.1257/jel.20191385

Van Vo, D., & Csapó, B. (2020). Development of inductive reasoning in students across school grade levels. *Thinking Skills and Creativity*, *37*(September), 100699. https://doi.org/10.1016/j.tsc.2020.100699

Vicedo-Cabrera, A. M., Scovronick, N., Sera, F., Royé, D., Schneider, R., Tobias, A., et al. (2021). The burden of heat-related mortality attributable to recent human-induced climate change. *Nature Climate Change*, *11*(6), 492–500. https://doi.org/10.1038/s41558-021-01058-x

23284277, 2024, 10, Downloaded from https://agupubs.onlinelibrary.wiley.com/doi/10.1029/2024EF004431 by Area Sistemi Dipart & Document, Wiley Online Library on [23/10/2024]. See the Terms and Conditions (https://onlinelibrary.wiley.com/terms-and-conditions) on Wiley Online Library for rules of use; OA articles are governed by the applicable Creative Commons License

Wear, D. N., & Prestemon, J. (2019). Spatiotemporal downscaling of global population and income scenarios for the United States. In A. Zia (Ed.) (Vol. *14*). https://doi.org/10.1371/journal.pone.0219242. *PLoS One* (7). e0219242.

Wilson, T., Grossman, I., Alexander, M., Rees, P., & Temple, J. (2022). Methods for small area population forecasts: State-of-the-Art and research needs. *Population Research and Policy Review*, *41*(3), 865–898. https://doi.org/10.1007/s11113-021-09671-6

Wittgenstein Centre Human Capital Data Explorer. (2018). Retrieved from https://dataexplorer.wittgensteincentre.org/wcde-v2/

Zafeiratou, A., Founda, G., Varotsos, S., Keramitsoglou, K., Varotsos, K. V., Sismanidis, P., et al. (2019). Spatial variability in the effect of high ambient temperature on mortality: An analysis at municipality level within the greater athens area. *International Journal of Environmental Research and Public Health*, *16*(19), 3689. https://doi.org/10.3390/ijerph16193689

Zhao, L., Oleson, K., Bou-Zeid, E., Scott Krayenhoff, E., Bray, A., Zhu, Q., et al. (2021). Global multi-model projections of local urban climates. *Nature Climate Change*, *11*(2), 152–157. https://doi.org/10.1038/s41558-020-00958-8

Zoraghein, H., & Brian, O. 'N. (2020). A spatial population downscaling model for integrated human-environment analysis in the United States. *Demographic Research*, *43*(December), 1483–1526. https://doi.org/10.4054/DemRes.2020.43.54

References From the Supporting Information

UNESCO-UIS. (2012). International standard classification of education ISCED 2011. Retrieved from http://www.uis.unesco.org

Wittgenstein Centre Data Explorer. (2018). Wittgenstein Centre for demography and global human capital. Retrieved from http://www.wittgensteincentre.org/dataexplorer

Statistics | Eurostat. (n.d.). Retrieved from https://ec.europa.eu/eurostat/databrowser/view/EDAT_LFSE_04/default/table?lang=en&category=educ.educ_outc.edat.edat1

23284277, 2024, 10, Downloaded from https://agupubs.onlinelibrary.wiley.com/doi/10.1029/2024EF004431 by Area Sistemi Dipart & Document, Wiley Online Library on [23/10/2024]. See the Terms and Conditions (https://onlinelibrary.wiley.com/terms-and-conditions) on Wiley Online Library for rules of use; OA articles are governed by the applicable Creative Commons License